# A SIMPLIFIED MODEL FOR EVALUATING eVTOL CONCEPTUAL DESIGNS AND WITH EXAMPLE RESULTS FOR THREE TYPES OF EVTOL AIRCRAFT CONFIGURATIONS

**Shawn Lim Kin Yip**
PhD candidate
kinyipsh001@e.ntu.edu.sg
Nanyang Technological University
Singapore

**Andy Koh Jun Hoong**
Graduate
andy0031@e.ntu.edu.sg
Nanyang Technological University
Singapore

**James Wang**
Professor
james.wang@ntu.edu.sg
Nanyang Technological University
Singapore

## Abstract

eVTOL Performance Analysis Tool, known as *ePERF* is a MATLAB-based analysis developed at NTU specifically for evaluating the performance of different types of eVTOL aircraft and is ideal for eVTOL aircraft conceptual and preliminary design phases. The framework is built to have a modular nature allowing for rapid trade studies of different sizing parameters, and it provides a representative performance evaluation of the eVTOL in all phases of flight. *ePERF* consists of three main modules: a rotary wing module, a drag estimation module for forward flight and an energy module for range calculation. Momentum theory is used for hover calculations. A component level drag build-up method is used for cruise calculations. The energy model considers the input battery parameters and results from the other two modules to compute the energy requirements of the eVTOL based on a given mission profile. The outputs of *ePERF* include the power and energy requirements for each flight phase, an estimated attainable range, as well as the velocity for best range. In this paper, the *ePERF* is explained and then it is used to estimate the performance for three different example eVTOL aircraft: *(A)* a Lift + Cruise type like Beta Technologies - Alia, *(B)* a tiltrotor type like Joby Aviation - S4, and *(C)* a fixed Lift + Tiltrotor type like Vertical Aerospace - VX4. The results show that reducing the structural weight of the eVTOL aircraft is one of the key factors in achieving best performance.

## Notation

### Acronyms

| | |
|---|---|
| AGL | Above Ground Level |
| ePERF | eVTOL Performance Analysis Tool |
| eVTOL | Electric Vertical Takeoff and Landing |
| MTGW | Maximum Takeoff Gross Weight, [kg] |
| UAM | Urban Air Mobility |

### Rotary Wing Model Calculations

| | |
|---|---|
| $A$ | Rotor disk area $[m^2]$ |
| $\rho$ | Density $[kg/m^3]$ |
| $T$ | Thrust $[N]$ |
| $P_{hover,ideal}$ | Ideal hover power required $[kW]$ |
| $P_{hover,actual}$ | Actual hover power required $[kW]$ |

### Drag Model Calculations

| | |
|---|---|
| $C_d$ | Overall drag coefficient [-] |
| $C_{d_0}$ | Parasite drag coefficient [-] |
| $C_{d_i}$ | Induced drag coefficient [-] |
| $k$ | Induced drag factor |
| $C_L$ | Lift Coefficient [-] |
| $C_{f,c}$ | Skin friction drag coefficient of component [-] |
| $\Phi_{f,c}$ | Form factor of component [-] |
| $S_{wet,c}$ | Wetted area of component $[m^2]$ |
| $C_{d,c}$ | Empirical drag coefficient of component based on its frontal area [-] |
| $S_{front,c}$ | Frontal area of component $[m^2]$ |
| $S_{wing,ref}$ | Reference wing area $[m^2]$ |
| $\vec{V}_{br}$ | Velocity for best range [m/s] |

### Energy Model Calculations

| | |
|---|---|
| $P_{segment,\ actual}$ | Power required to execute flight segment $[kW]$ |
| $t_{segment}$ | Time taken to complete flight segment $[s]$ |
| $E_{segment,\ actual}$ | Actual energy needed to complete flight segment $[kJ]$ |
| $W_{eVTOL}$ | Weight of eVTOL aircraft [N] |
| $\eta_{overall}$ | Overall efficiency of aircraft [-] |

## 1. Introduction and Previous Work

In recent years, urban traffic has become a dire issue for numerous large urban cities around the world and has caused trillions of dollars in the form of energy and time, as well as increased air pollution [1]. One prospective solution is to expand traditional transportation network into the 3D space using Urban Air Mobility (UAM) and electric

Vertical Take-Off and Landing (eVTOL) aircraft. However, recent articles have highlighted several evolving challenges in its adoption and implementation including air traffic management, community acceptance, infrastructure, safety, flight range, noise and regulations [2]–[4]. Several studies have shown that a significant part of these challenges is associated with the design, architecture and sizing of eVTOL aircraft which affects the vehicle emissions, performance, operations, economics and certification for UAM [5], [6].

eVTOL aircraft designers have proposed various configurations and combinations of fixed and rotary wing propulsive architectures and technologies such as distributed electric propulsion, multi-rotors, ducted fans, vectored propulsion and fixed-wings designs in different orientations and configurations [7]–[10]. This leads to an aircraft design space with a multitude far greater than conventional aircraft. Hence, there is a need to have a simplified method to rapidly evaluate and compare the various combinations of eVTOL technologies and architectures that will guide eVTOL conceptual design choices to improve flight performance and efficiency quickly and easily.

Notable works in this area include Reference [11], which compared the aerodynamic performance and handling qualities for four different eVTOL configurations in cruising flight using AVL and CFD, and presented the respective pros and cons for each configuration. In another study, Bacchini and Cestino compared various aircraft configurations using analytical equations to model multi-copter, Lift + Cruise and vectored thrust configurations [12]. Both studies highlighted the impact of aircraft design choices that affects the aircraft performance and efficiency. Other studies by Johnson and Silva also compared various concept vehicles based on quadrotors, side-by-side helicopter, tiltwing and Lift + Cruise configurations using sophisticated NDARC and CAMRAD II tools [13], [14].

Their results highlighted the critical research areas required for eVTOL development including propulsive efficiency, aircraft performance, aerodynamic interactions, aircraft design, operational effectiveness, and cost. Additionally, Brown and Harris analyzed four eVTOL configurations including Lift + Cruise, compound helicopter, tiltwing and tiltrotor using geometric programming to compare the noise performance of the various eVTOL configurations [15]. Their findings show that parameters such as number of rotors, number of rotor blades, rotor solidity, blade thickness-to-chord ratio and maximum mean lift coefficient have the strongest influence on the noise emitted by the different configurations.

This paper aims to facilitate doing competitive analysis and help the development of new eVTOL aircraft by presenting a newly developed versatile tool to enable rapid trade studies by calculating the performance of different types of eVTOL aircraft based on geometrical and mission critical parameters, and loss factors. The tool is intended to be used in the conceptual and preliminary design phases where detailed variables may not be available to the eVTOL designer. The code is developed as modular sections to allow greater flexibility and understanding for eVTOL designers to perform rapid trade study analyses of different design parameters for different eVTOL configurations and provide a representative performance evaluation of the eVTOL aircraft in every segment of flight.

## 2. Description of ePERF

The *ePERF* framework is shown in Figure 1, where the eVTOL Performance Tool, known as *ePERF*, consists of three main modules: a rotary wing model for hover flight, a drag model for steady state cruise and an energy model for estimation of the achievable range of the eVTOL design. *ePERF* utilizes only four main sets of input variables for an analysis, namely the design dimensions, the efficiency factors, the battery parameters, and the desired mission profile. The baseline values used are derived through various existing resources and previous studies.

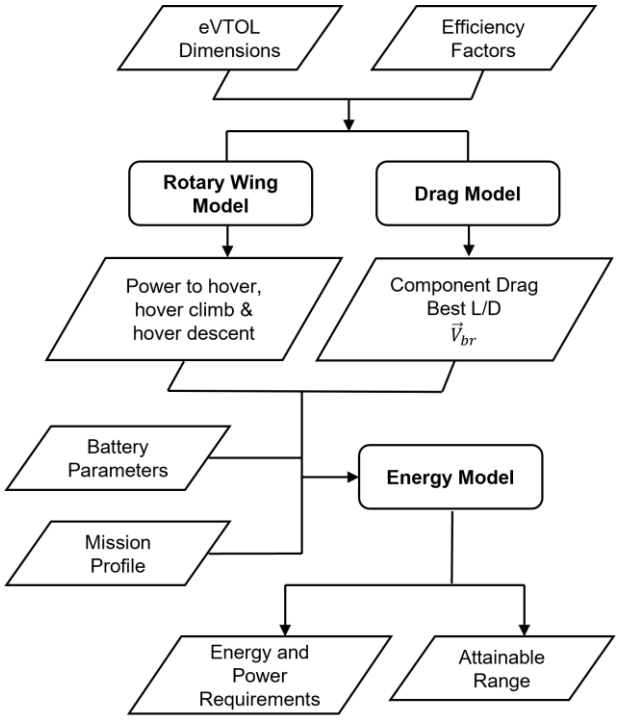


Figure 1. Flowchart showing required inputs, generated outputs, and modules in *ePERF* analysis tool

### 2.1. eVTOL Input Parameters

Three different eVTOL aircraft are chosen to demonstrate *ePERF* capabilities and to represent three different categories of eVTOL aircraft. The dimensions and battery parameters of these three eVTOLs are shown

in Table 1. It should be noted that we do not claim the results presented in this study are intended to be exact performance values of the following three aircraft shown in Figure 2. The presented results are only used to project the performance differences among three generic types of eVTOL aircraft. For the rest of the paper, the three eVTOL configurations, the Lift + Cruise, the tiltrotor, and the Lift + Tiltrotor will be referred to as configurations: *eVTOL (A)*, *eVTOL (B)*, and *eVTOL (C)* respectively.

Table 1. Specified input parameters used in *ePERF* analysis for *eVTOL (A)*, *(B)* and *(C)*

| Specified Parameters | *eVTOL (A)* | *eVTOL (B)* | *eVTOL (C)* |
|---|---|---|---|
| Configuration Type | Lift + Cruise | Tiltrotor | Lift + Tiltrotor |
| Maximum Takeoff Gross Weight $(kg)$ | 3175 | 2177 | 3175 |
| Number of Passengers | 6 | 5 | 5 |
| Fuselage Length $(m)$ | 7.8 | 6.4 | 10.5 |
| Fuselage Diameter $(m)$ | 1.7 | 1.6 | 1.8 |
| Wingspan $(m)$ | 15.2 | 10.5 | 15 |
| Wing Area $(m^2)$ | 19.8 | 11.6 | 26.8 |
| Empennage Wetted Area $(m^2)$ | 8.7 | 12.4 | 13.7 |
| Number of Rotors | 4 | 6 | 8 |
| Lift Rotor Diameter $(m)$ | 3.9 | 3.1 | 3.1 |
| Wing Loading $(N/m^2)$ | 1573 | 1841 | 1162 |
| Disk Loading $(N/m^2)$ | 648.5 | 471.6 | 491.0 |
| Available Energy $(kWh)$ | 230 | 160 | 230 |

*eVTOL (A)*: a Lift + Cruise, similar to [16]

*eVTOL (B)*: a Tiltrotor, similar to [17]

*eVTOL (C)*: a Lift + Tiltrotor, similar to [18]

Figure 2. The *ePERF* code is used to analyze three different eVTOLs that loosely resemble: *(A)* Beta Technologies Alia, *(B)* Joby Aviation S4, and *(C)* Vertical Aerospace VX4

### 2.2. Efficiency Factors

Efficiency factors are employed to provide a simple way to correct for non-ideal effects that are not accounted for in theoretical calculations. Table 2 lists the six efficiency factors required by *ePERF* for the performance estimation during hover flight and cruise phases. These factors are set based on existing literature and standardized across different eVTOL aircraft for a fair comparison of their respective design configurations.

Table 2. Standardized Efficiency Factors used in *ePERF* analysis for *eVTOL (A)*, *(B)* and *(C)*

| Phase of Flight | Specified Factors | Specified Values |
|---|---|---|
| Hover | Rotor Figure of Merit | 0.78 |
| | Rotor Power Correction | 0.8 |
| Cruise | Electrical Efficiency | 0.9 |
| | Oswald Efficiency | 0.75 |
| | Propulsive Efficiency | 0.85 |
| | Overall Efficiency | 0.765 |

### 2.3. Standardized Mission Profile

Figure 3 presents a baseline main and reserve mission profile based on the proposed requirements by Uber Air [19]. Each mission profile is defined by seven main flight segments: (1) takeoff hover, (2) transition from hover to forward flight, (3) cruise climb, (4) cruise, (5) cruise descent, (6) transition from forward flight to hover, and (7) hover descent.

The vertical speeds and specified altitudes are kept constant for each segment (excluding cruise), and each eVTOL aircraft is assumed to spend the same amount of time during each maneuver. The cruise duration is determined by each eVTOL's available energy, based on the power required for cruise and its velocity at best range $\vec{V}_{br}$. This allows for an equal comparison of the aircraft's performance in terms of energy required per flight segment and the attainable mission range. The eVTOL is also required to have sufficient reserves to complete a reserve mission in the event of failure, as shown in Figure 3 (b). For the reserve cruise segment, the reserve range is set at 10% of the main mission range.

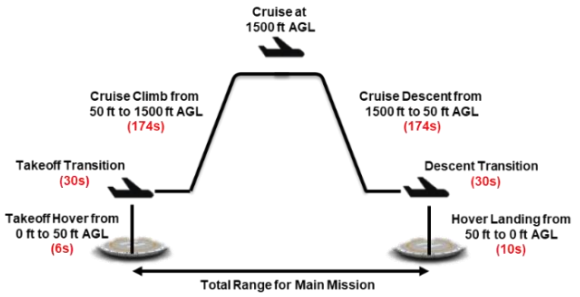


| Segment | Vertical Speed | Horizontal Speed | AGL Ending Altitude | Time taken (s) |
|---|---|---|---|---|
| Takeoff Hover | +2.54 m/s | 0 | 15.24 m | 6 |
| Takeoff Transition | 0 | 0 to $\vec{V}_{br}$ | 15.24 m | 30 |
| Cruise Climb | +2.54 m/s | $\vec{V}_{br}$ | 457.2 m | 174 |
| Cruise | 0 | | 457.2 m | TBD |
| Cruise Descent | -2.54 m/s | | 15.24 m | 174 |
| Descent Transition | 0 | $\vec{V}_{br}$ *to* 0 | 15.24 m | 30 |
| Hover Descent | -1.52 m/s | 0 | 0 | 10 |

(a) Main Mission Profile

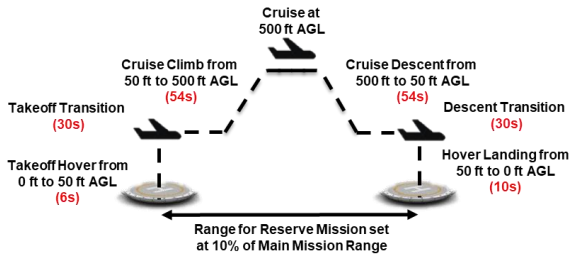


| Segment | Vertical Speed | Horizontal Speed | AGL Ending Altitude | Time taken (s) |
|---|---|---|---|---|
| Takeoff Hover | +2.54 m/s | 0 | 15.24 m | 6 |
| Takeoff Transition | 0 | 0 to $\vec{V}_{br}$ | 15.24 m | 30 |
| Cruise Climb | +2.54 m/s | $\vec{V}_{br}$ | 457.2 m | 174 |
| Cruise | 0 | | 457.2 m | TBD |
| Cruise Descent | -2.54 m/s | | 15.24 m | 174 |
| Descent Transition | 0 | $\vec{V}_{br}$ *to* 0 | 15.24 m | 30 |
| Hover Descent | -1.52 m/s | 0 | 0 | 10 |

(b) Reserve Mission Profile

Figure 3. Specifications for main and reserve eVTOL mission profile used in energy model

## 3. Methodology

In this section, an overview of the three modules in *ePERF*, namely the rotary wing, drag and energy models, is presented.

### 3.1. Rotary Wing Power Module

In the rotary wing power model, the power required for hover, hover climb, and hover descent are calculated based on momentum theory. The ideal hover thrust required for each flight phase is equal to the eVTOL weight and is given by equation (1). The ideal power to hover climb and hover descent are empirically estimated using the methodology presented in [20]. These ideal results obtained are each adjusted by their respective correction factors to account for the rotor figure of merit as well as the additional electrical and interference losses. For a fair comparison between designs, these correction factors are set at an effective value of 0.624.

$$P_{hover,ideal} = \sqrt{\frac{T^3}{2\rho A}} \quad -(1)$$

$$P_{hover,actual} = \frac{P_{hover,ideal}}{0.624} \quad -(2)$$

### 3.2. Fixed Wing Drag Module

In the fixed wing drag model, the aerodynamic efficiency of the eVTOL is evaluated in steady-state subsonic cruise. The lift required is equal to the eVTOL weight. The total drag acting on the eVTOL depends on the amount of parasite and induced drag and is given by equation (3). To improve the drag calculations, especially for eVTOL aircraft that has multiple external parts and bodies, the component build-up method by Raymer, given by equation (4), is used for parasite drag modelling of the following components: wing, fuselage, empennage, booms, nacelles and propellers [21].

For induced drag, the Oswald span efficiency method is used. As parasite drag increases and induced drag decreases with flight velocity, there exists an optimal cruise velocity where the lift-to-drag ratio is the highest. Using the innate MATLAB optimizer in drag model, this optimal point, known as the cruise velocity for best range, $\vec{V}_{br}$, is automatically solved.

$$C_d = C_{d_0} + kC_L{}^2 \quad -(3)$$

$$C_{d_0} = \frac{\sum(C_{f,c} \cdot \Phi_{f,c} \cdot S_{wet,c}) + \sum(C_{d,c} \cdot S_{front,c})}{S_{wing,ref}} \quad -(4)$$

### 3.3. Energy Consumption Module

In the energy model, the outputs from the rotary wing power and fixed wing drag models are used in conjunction with battery input parameters to estimate the total attainable range of the eVTOL based on the mission profile presented in Figure 3. The battery energy capacities that have been selected for this study are: 160 kWh for *eVTOL (B)* and 230 kWh for both *eVTOL (A)* and *eVTOL (C)* respectively. For example, if the battery has a specific energy of 250 Wh/kg at the pack level, then the weight for a 230 kWh would be 920 kg. A detailed breakdown of the energy and power required for each phase of flight was first derived to calculate the eVTOL's energy consumptions. The methodology used to determine the energy required for each phase is summarized in Table 3.

The total attainable range of each eVTOL is a function of its specified battery energy capacity, remaining energy for cruise phase, cruise power, and cruise velocity. The energy remaining for cruise phase for each eVTOL is first obtained by subtracting the total energy required for all other phases from its respective specified battery energy capacity. Next, the time spent in cruise is computed by dividing the remaining energy by its power requirement for cruise. The total attainable range of each eVTOL is the product of the time spent in cruise and its cruise velocity.

Table 3. Summary of energy and power calculations

| | |
|---|---|
| Take-off Hover | $E_{hc,actual} = P_{hc,actual} \cdot t_{hc}$ |
| Hover & Descent Transition | $P_{transition} = P_{hover,actual}$<br>$E_{transition} = P_{transition} \cdot t_{transition}$ |
| Cruise Climb | (For vertical portion of cruise climb only)<br>$E_{cc,vertical} = \frac{W_{eVTOL} \cdot h_{cc}}{\eta}$<br>$P_{cc,vertical} = \frac{E_{cc,vertical}}{t_{cc,vertical}}$ |
| Cruise | $E_{cruise} = \frac{W_{eVTOL} \cdot Range}{L/D} / \eta_{overall}$<br>$P_{cruise} = \frac{W_{eVTOL} \cdot \vec{V}_{cruise}}{L/D} / \eta_{overall}$ |
| Cruise Descent | (For vertical portion of cruise descent only)<br>$P_{cd} \approx 0 \rightarrow E_{cd} = 0$ |
| Hover Descent | $E_{hd,actual} = P_{hd} \cdot t_{hd}$ |

## 4. eVTOL Model Results

This section presents a comparison of the predicted performance results among the three eVTOL aircraft using the three modules in *ePERF*. These results obtained are based on the parameters specified in Table 1.

### 4.1. Rotary Wing Modeling of Vertical Flight

The rotary wing model was first used to predict the power required in hover flight segments, including the hover, hover climb and hover descent, for each eVTOL aircraft at different maximum takeoff gross weights (MTGW). Table 4 contains the variables used in the rotary wing model calculations for the three aircraft. The hover performance results are summarized and compared for different maximum takeoff gross weights (MTGW) in Figure 4. Each data point varies by 100 $kg$ in the x-axis. This variation in aircraft weight represents a change in payload for each passenger carried from 0 up to 6 passengers.

The power required is highest in hover climb segment due to the increased thrust required to accelerate the aircraft vertically, followed by hover and lowest in hover descent phase. The results shows that *eVTOL (B)* requires the least power in hover flight, followed by *eVTOL (C)*, with *eVTOL (A)* requiring the most power. In hover, the power required squared is proportional to the disk loading and proportional to the cube of the aircraft weight. For aircraft at the same MTGW, a lower rotor disk loading is desirable for hover flight. *eVTOL (B)* has a similar rotor disk loading to *eVTOL (C)*, but *eVTOL (B)* requires much lower absolute power for hover flight due to its lower weight.

Table 4. Rotor disk loading values based on eVTOL MTGW and Rotor Disk Areas for *eVTOL (A)*, *(B)* and *(C)*

| Aircraft | eVTOL MTGW (kg) | Estimated Rotor Disk Area ($m^2$) | Rotor Disk loading ($N/m^2$) |
|---|---|---|---|
| *eVTOL (A)* | 3175 | 48.03 | 648.5 |
| *eVTOL (B)* | 2177 | 45.29 | 471.6 |
| *eVTOL (C)* | 3175 | 63.44 | 491.0 |

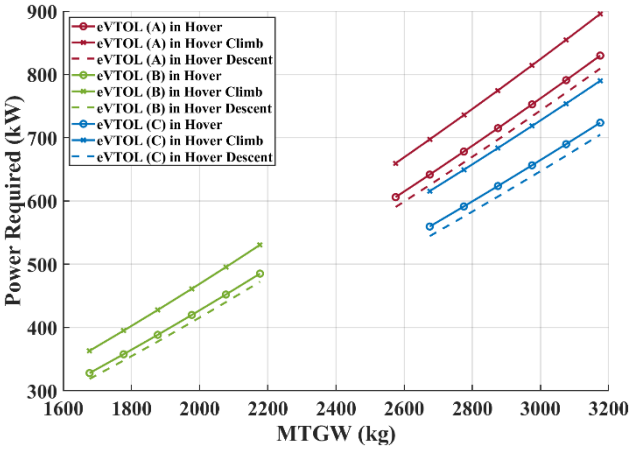


Figure 4. Comparison results of power required for different hover phases and eVTOL MTGW between *eVTOL (A)*, *(B)* and *(C)* using the rotary wing model

### 4.2. Drag Modeling of Forward Flight

The individual component drag breakdown for each eVTOL during steady-state cruise at their MTOW and $\vec{V}_{br}$ is shown in Table 5. Across all three eVTOLs, the induced drag contributes the largest portion of total drag at 48% whereas the interference drag between the wing and fuselage contributes the smallest portion at around 0.3%. The drag percentages for general aircraft components are found to be fairly similar across the three configurations.

Table 5. Drag breakdown of each individual component

| Defined Components | *eVTOL (A)* | *eVTOL (B)* | *eVTOL (C)* |
|---|---|---|---|
| Fuselage | 6.9 % | 10.4 % | 8.6 % |
| Wing Parasite | 12.6 % | 13.6 % | 14.4 % |
| Wing Induced | 48.3 % | 48.4 % | 47.9 % |
| Wing Interference | 0.2 % | 0.3 % | 0.4 % |
| Empennage | 6.5 % | 8.9 % | 8.4 % |
| Landing Gear | 4.6 % | 6.0 % | - |
| Booms | 4.7 % | - | 6.8 % |
| Stationary Propellers | 16.2 % | - | 13.5 % |
| Nacelles of Tiltrotors | - | 12.4 % | - |

It is also observed that the additional eVTOL-specific components resulted in comparatively higher drag contributions at 12% of total drag for *eVTOL (B)* and around 20% of total drag for both *eVTOLs (A)* and *(C)*. For *eVTOL (B)*, the components include the nacelles for the horizontal tiltrotors. For *eVTOL (A)* and *(C)*, these components include the booms as well as the blades and spinners of stationary propellers. The booms are predicted to contribute a smaller portion of total drag (between 5% and 7%) due to their streamlined shape. This observation points towards a significant trade-off in cruise performance in exchange for VTOL capabilities.

Results from the drag model are used to compare the aerodynamic efficiency and performance of each eVTOL in cruise flight. The optimal cruise velocity for best range, corresponding peak lift-to-drag ratio and required power to cruise for each eVTOL model at MTGW are compared in Table 6.

Table 6. eVTOL output parameters from drag model

| | *eVTOL (A)* | *eVTOL (B)* | *eVTOL (C)* |
|---|---|---|---|
| $MTGW\ (kg)$ | 3175 | 2177 | 3175 |
| $S_{wing}\ (m^2)$ | 19.82 | 11.58 | 26.76 |
| Wing Loading $(N/m^2)$ | 1573 | 1841 | 1162 |
| $\vec{V}_{br}(m/s)$ | 53.7 | 63.5 | 52.9 |
| $L/D\ @\ \vec{V}_{br}$ | 14.33 | 13.42 | 13.36 |
| $P_{cruise}\ @\ \vec{V}_{br}\ (kW)$ | 152.3 | 132.0 | 161.1 |

The analysis has shown a higher $\vec{V}_{br}$ is predicted for *eVTOL (B)* than for *eVTOL (A)* and *(C)*. This is attributed to the higher wing loading that *eVTOL (B)* has compared to the other two aircraft. A higher $\vec{V}_{br}$ consequently yields faster flight time between missions. In terms of cruise aerodynamic efficiency, *eVTOL (A)* is predicted to be the most efficient with the highest peak lift-to-drag (L/D) ratio of 14.4. Both *eVTOL (B)* and *(C)* each have similar lower peak L/D ratios.

The power to cruise at $\vec{V}_{br}$ is the most indicative parameter for the comparison of overall cruise performance as it accounts for the MTGW, aerodynamic efficiency and cruise velocity for each eVTOL aircraft. *eVTOL (B)* is predicted to require the lowest power to cruise at $\vec{V}_{br}$ because of its lowest weight among the three aircraft. This highlights the importance of reducing aircraft weight in achieving better cruise performance.

### 4.3. Mission based Energy Modeling

The detailed breakdown of the energy and power required for each eVTOL at its specified MTGW for different mission flight segments is presented in Figure 5.

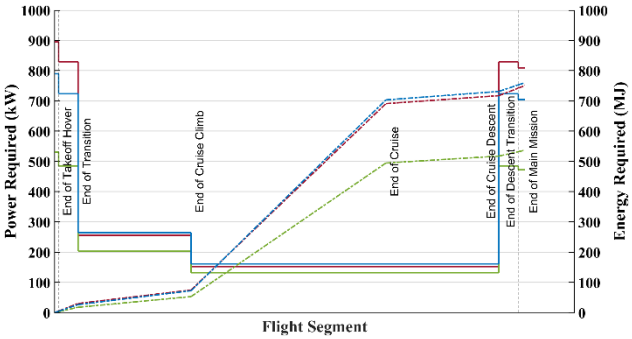


Figure 5. Power (solid line) and energy (dotted line) required against flight segment for *eVTOL (A)* (red line), *eVTOL (B)* (green line) and *eVTOL (C)* (blue line) at their specified MTGW and $\vec{V}_{br}$

For a typical flight mission, vertical flight segments require the highest amount of power, followed by cruise climb and the lowest amount of power is required during cruise. For the two eVTOLs with the MTGW of 3175 kg, their power requirements for hover climb are found to be between five to six times greater than the power requirements for cruise. Thus, a typical eVTOL mission profile aims to maximise the time spent in cruise and minimise the time spent in hover flight phases to achieve the best range performance.

Table 7 compares the main and reserve mission cruise duration for each eVTOL to fully deplete its defined battery energy, inclusive of the reserve mission requirements. An average of 85% of the mission time is spent in the cruise phase for the main and reserve mission for all three eVTOLs.

Table 7. Time spent in vertical flight and cruise flight segments for *eVTOL (A)*, *(B)* and *(C)*

| | *eVTOL (A)* | *eVTOL (B)* | *eVTOL (C)* |
|---|---|---|---|
| MTGW (kg) | 3175 | 2177 | 3175 |
| Total Energy (kWh) | 230 | 160 | 230 |
| Vertical Flight | 424 s | 424 s | 424 s |
| Cruise | 3708 s | 3003 s | 3575 s |
| Vertical Flight (R) | 184 s | 184 s | 184 s |
| Cruise (R) | 371 s | 300 s | 358 s |

The energy spent in each flight segment is a function of both the power requirements and the duration of that segment, which in turn affects the maximum aircraft range. Table 8 compares the proportion of energy used in cruise and vertical flight phases for each aircraft. Across the three aircraft, the proportion of energy used in each phase is fairly similar, with the bulk of the energy available used in cruise. This is due to the equal duration constraint applied for each hover flight segment.

Table 8. Proportion of energy used in cruise and vertical flight phases for *eVTOL (A)*, *(B)* and *(C)*

| | *eVTOL (A)* | *eVTOL (B)* | *eVTOL (C)* |
|---|---|---|---|
| MTGW (kg) | 3175 | 2177 | 3175 |
| Total Energy (kWh) | 230 | 160 | 230 |
| Cruise | 74.6% | 76.8% | 76.3% |
| Vertical Flight | 9.8% | 8.6% | 8.8% |
| Cruise (R) | 7.5% | 7.7% | 7.6% |
| Vertical Flight (R) | 8.2% | 6.9% | 7.2% |

## 5. Sensitivity Studies

Several sensitivity studies were also conducted using ePERF to understand the importance of different parameters on the overall performance results obtained for eVTOL aircraft. These parameters include: MTGW, cruise velocity, specified mission range and battery capacity.

### 5.1. Variation of MTGW

For the MTGW sensitivity study, only the weight inputs for each eVTOL aircraft are varied. This allows for the study on how the eVTOL weight affects the aircraft performance, that is especially useful to determine an optimal configuration among the list of aircraft for a given weight class. All other inputs into *ePERF* were kept constant based on the parameters shown in Table 1. The weight inputs are swept at an interval of 100 kg to represent the variation in weight of each additional passenger from an empty configuration to that of a fully loaded configuration.

A case where *eVTOL (B)* has a fully loaded weight of 3175 kg was also added to the existing set of data, with all other parameters being kept constant. The authors deem that by adding a set of result for the *eVTOL (B)* with the same weight as the other aircraft would permit a fairer comparison among the configurations. The result is labelled as *eVTOL (B-3175)*. The limit of 3175 kg is chosen is based on the EASA maximum weight certification limit for an eVTOL aircraft. This case investigates the sensitivity of the performance of *eVTOL (B)* to weight growth, which was originally sized for a lower weight of 2177 kg.

The hover performance results obtained for *eVTOL (B-3175)* is compared with *eVTOL (B)* in Figure 6. The variables used in the rotary wing calculations for the two cases are listed in Table 9. The results show the ranking of power required from the lowest to highest value following the order of *eVTOL (B)*, *eVTOL (C)*, *eVTOL (A)* and *eVTOL (B-3175)*. *eVTOL (B)* and *eVTOL (B-3175)* differ in mass by 998 kg. This leads to an increase in rotor disk loading of 216.1 N/m$^2$ and much poorer hover performance for *eVTOL (B-3175)*. The power required for each hover phase is observed to increase by around 1.7 times.

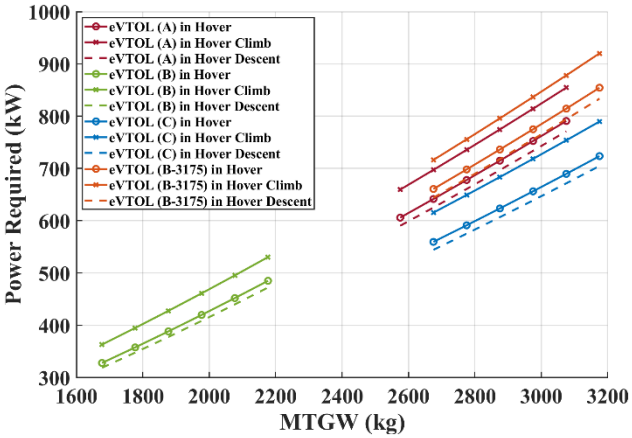


Figure 6. Comparison results of power required for different hover phases and eVTOL MTGW between *eVTOL (B)* and *eVTOL (B-3175)* generated using the rotary wing model

Table 9. Rotor disk loading values based on eVTOL MTGW and rotor disk areas for *eVTOL (B)* and *eVTOL (B-3175)*

| Specified Aircraft | eVTOL MTGW (kg) | Estimated Rotor Disk Area (m$^2$) | Rotor Disk loading (N/m$^2$) |
|---|---|---|---|
| *eVTOL (B)* | 2177 | 45.29 | 471.6 |
| *eVTOL (B-3175)* | 3175 | 45.29 | 687.7 |

The cruise performance results are then computed using the energy model in *ePERF* for each eVTOL across their assumed weight variations. Figure 7 shows the combined plot of main mission range (represented by solid lines) and power to cruise (represented by dotted lines) against MTGW for each eVTOL. The main mission range is a function of the aerodynamic efficiency, battery energy available and eVTOL mass. The results show the ranking

of mission range from the highest to lowest value following the order of *eVTOL (B)*, *eVTOL (A)*, *eVTOL (C)* and *eVTOL (B-3175)*. At their baseline MTGW, the predicted ranges of *eVTOL (A)*, *(B)* and *(C)* are similar at around 215 km. This indicates that the overall cruise performance is comparable among these three aircraft for their respective designed weight classes.

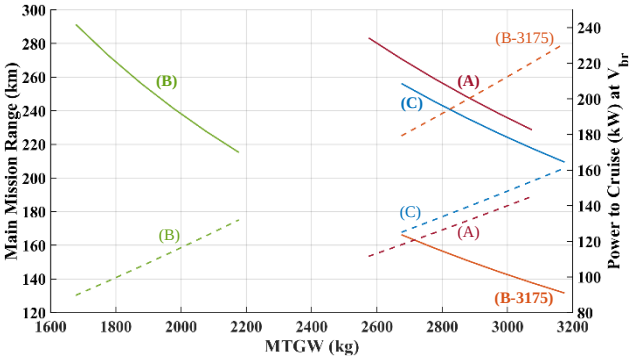


Figure 7. MTGW sensitivity study for the main mission range (solid lines) and rower to cruise (dotted lines) for *eVTOL (A)* (red lines), *eVTOL (B)* (green lines), *eVTOL (B-3175)* (orange line) and *eVTOL (C)* (blue lines)

Across the four eVTOL aircraft, it is observed that an increase in MTGW leads to a corresponding increase in power to cruise required and a decrease in attainable main mission range. Every 100 kg increase in mass is projected to decrease attainable range by approximately 10 to 15 km for the various eVTOL configurations, with *eVTOL (B)* showing the largest decrease.

Comparing between *eVTOL (B)* and *eVTOL (B-3175)*, there is a drastic decrease in attainable main mission range by around 110 km at their respective MTGWs. The power to cruise for *eVTOL (B-3175)* is predicted to increase by roughly 1.5 times that of *eVTOL (B)* and having the highest power consumption among the other configurations, thereby reducing the energy available for the cruise segment. Hence for the cruise performance, *eVTOL (B-3175)* is the worst among all cases. Thus, any increase in the weight of *eVTOL (B)* will require a separate optimization of the overall design parameters of the eVTOL to ensure comparable performance with the other eVTOL aircraft.

### 5.2. Variation of Velocity

The optimal cruise velocity for each eVTOL aircraft will be different depending on its eVTOL configuration. It is important to study how the changes in cruise velocity could affect the cruise performance of an eVTOL aircraft in terms of range and power requirements. This study allows for the identification of configurations that allow for a higher cruise velocity, enabling them to complete their mission quicker.

Figure 8 illustrates the combined plot of main mission range (represented by solid lines) and power to cruise (represented by dotted lines) against cruise velocity for each eVTOL aircraft at their specified MTGW. Both sets of plots are observed to follow a parabolic shape due to the effects of high parasitic drag at low speeds while having high induced drag at high speeds.

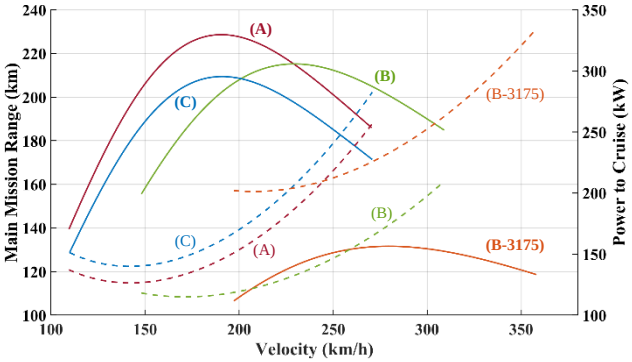


Figure 8. Cruise velocity sensitivity study for the main mission range (solid lines) and power to cruise (dotted lines) against velocity for *eVTOL (A)* (red lines), *eVTOL (B)* (green lines), *eVTOL (B-3175)* (orange line) and *eVTOL (C)* (blue lines)

*eVTOL (A)* is able to achieve the highest maximum range of 220 km among the different aircraft at a velocity of 193 km/h. It is noted that its power to cruise is not minimum at this velocity. Its minimum power to cruise velocity is lower at around 150 km/h. More specifically, the velocity for the theoretical minimum power can be taken to be 0.76 times that of the velocity for best range.

The results show the ranking of cruise velocity from the highest to lowest value for the maximum range following the order of *eVTOL (C)*, *eVTOL (A)*, *eVTOL (B)* and *eVTOL (B-3175)*. At velocities lower than 200 km/h, both *eVTOL (A)* and *(C)* outperform *eVTOL (B)* in terms of main mission range. At velocities higher than 200km/h, *eVTOL (B)* begins to outperform *eVTOL (C)* but not *eVTOL (A)*. For velocities higher than 225 km/h, *eVTOL (B)* is noted to have the best performance. This means that tiltrotor configuration in *eVTOL (B)* is ideal for missions where high cruise velocity is prioritized.

Comparing between *eVTOL (B)* and *eVTOL (B-3175)*, *eVTOL (B-3175)* has poorer cruise performance, achieving only a maximum main mission range of around 130 km. This reinforces the argument that the design for *eVTOL (B)* was optimized and designed for a lower weight class as compared to *eVTOL (A)* and *(C)*.

### 5.3. Variation of Range - Intracity, Intercity & Regional

With many eVTOL targeted for deployment for various applications that are range dependent, it is important to study the effect on how the achievable range for the different aircraft configurations could affect the performance and efficiency. The authors have classified the typical range terms for intracity, intercity and regional with distances under 50 km, 150 km, and 300 km respectively. Figure 9 shows the combined power and energy requirements against time for each eVTOL at their specified MTGWs for different mission ranges: intracity, intercity and regional for an entire mission.

Comparing *eVTOL (B)* to both *eVTOL (A)* and *(C)*, eVTOL (B) consumes less power in hover and cruise because of lower MTGW. Comparing *eVTOL (A)* and *(C)* and *eVTOL (B-3175)* which have the same MTGW, *eVTOL (A)* requires lower power to cruise at $\vec{V}_{br}$ whereas *eVTOL (C)* requires lower power to perform its hover phases. The plotted time required to complete each mission is dependent on the velocity for best range for each eVTOL. *eVTOL (B)* which has the highest $\vec{V}_{br}$ requires the shortest time to achieve the specified mission ranges. The results show the ranking of energy required from the lowest to highest value remains the same for any given ranged mission following the order of *eVTOL (B)*, *eVTOL (A)*, and *eVTOL (C)*.

All three eVTOLs have sufficient energy to complete both the intracity and intercity missions with reserves remaining. However, for the regional missions, it still poses a challenge and will require improvements to battery technologies or lower power requirements to become achievable.

For intracity ranges, *eVTOL (A)* and *eVTOL (C)* are observed to have comparable mission energy requirements. The energy requirements are still highly influenced by the hover performance of the eVTOL aircraft due to the relatively shorter time spent in cruise.

For intercity ranges, the mission energy requirements become more dependent on the cruise performance of the eVTOL aircraft. *eVTOL (A)* begins to outperform *eVTOL (C)* because of its higher aerodynamic efficiency even though it has lower hover efficiency.

However, for intracity and intercity ranges, *eVTOL (B)* is still the frontrunner in terms of low mission energy requirements due to its much lower MTGW specified at 2177 kg. If *eVTOL (B)* can truly achieve a MTGW of 2177 kg then its range is as good as the much heavier *eVTOL (C)*.

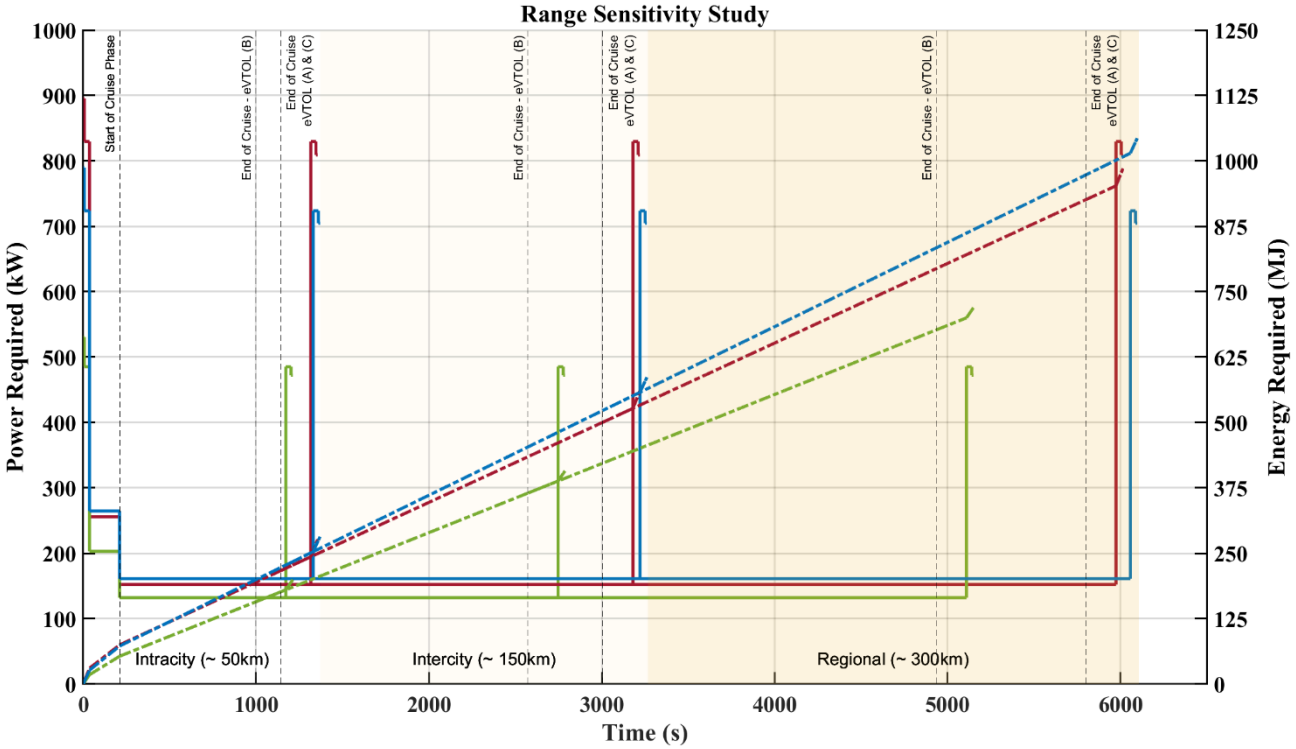


Figure 9. Range sensitivity study for the power required (solid line) and energy required (dotted line) against time for *eVTOL (A)* (red line), *eVTOL (B)* (green line) and *eVTOL (C)* (blue line)

### 5.4. Battery Capacity - 150 kWh, 250 kWh, 450 kWh

As battery technology improves in the coming years, it is necessary to study and forecast how the improvements in battery capacities that will be available for use in eVTOL could affect the eVTOL performance. This study compares the projections of the possible range achievable for the various eVTOL configurations with different pre-defined battery capacity. The authors have specified 3 different battery capacities based on the current, upcoming, and future development in battery technology with capacities of 150 kWh, 250 kWh and 450 kWh, respectively. Figure 10 shows the combined power and energy requirements against time for each eVTOL at their specified MTGWs with different battery capacities for an entire mission.

All three eVTOLs have achieved increased ranges from the increase battery capacities. As the hover properties of all the eVTOL aircraft remains unchanged, at their respective weights, it allows for greater energy available for cruise thereby extending the achievable ranges with an increase in battery capacity. Since *eVTOL (B)* has the lowest hover and cruise power requirement, it maintains its position on top of the other eVTOL aircraft in terms of achievable range. As for *eVTOL (A)* which requires lower power to cruise at $\vec{V}_{br}$ while *eVTOL (C)* requires lower power to perform its hover phases. An increase in batteries capacities, favors designs with highly efficient aerodynamic properties. Hence, it is necessary to observe the effect of the battery capacities changes for each configuration.

The achievable main mission ranges for the three aircraft with different specified battery capacities are recorded in Table 10. Across the specified battery capacities, the calculated results indicate that the ranking for mission range in descending order consistently follows the order of *eVTOL (B)*, *eVTOL (A)* and *eVTOL (C)*. However, due to the much lower MTGW of *eVTOL (B)*, it may not be able to carry onboard the 250 kWh of battery while the larger and heavier *eVTOLs (A)* and *(C)* can. If we were to assume the specific energy at the battery pack level is 250 Wh/kg, then it is likely that the *eVTOL (A)* and *(C)* could carry 250 kWh of battery (which is 1000 kg and roughly 31.5% of their MTGW), while *eVTOL (B)* may only carry 686 kg of battery (31.5% of 2177 kg) which equates to 171.5 kWh. Regardless, the cruise performance of an eVTOL aircraft should be prioritized over the hover performance when designing for maximum attainable range. This means try to design eVTOLs to require the minimal amount of cruise power.

Table 10. Achievable main mission ranges for each eVTOL aircraft at different specified battery capacities

| Battery Capacity | *eVTOL (A)* | *eVTOL (B)* | *eVTOL (C)* |
|---|---|---|---|
| 150 kWh | 109.7 km | 178.5 km | 106.1 km |
| 250 kWh | 225.0 km | 335.9 km | 213.4 km |
| 450 kWh | 455.7 km | 650.5 km | 428.2 km |

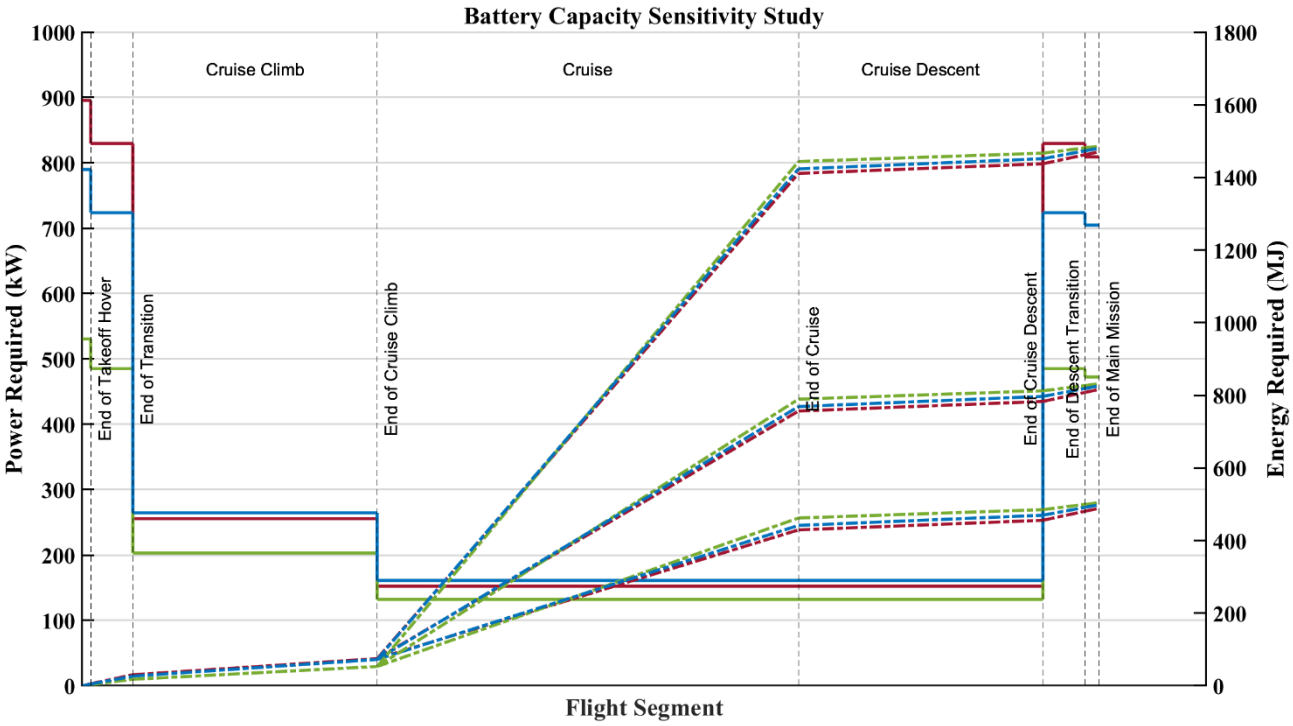


Figure 10. Battery capacity sensitivity study for the power required (solid line) and energy required (dotted line) against time for *eVTOL (A)* (red line), *eVTOL (B)* (green line) and *eVTOL (C)* (blue line)

## 6. Conclusion

The *ePERF* tool is a new analytical tool that has been developed specifically to evaluate eVTOL aircraft designs in terms of hover and aerodynamic efficiencies and provide a breakdown of the estimated energy required for each segment of the eVTOL flight. The *ePERF* is aimed to help researchers, aircraft designers and companies in conducting benchmark studies of different eVTOL configuration, in conducting trade studies of eVTOL aircraft geometric parameters, and for evaluating new eVTOL architectures during conceptual and preliminary design phases. Three representative eVTOL aircraft that roughly resemble three eVTOL aircraft: *(A)* Beta Technologies - Alia, *(B)* Joby Aviation - S4 and *(C)* Vertical Aerospace - VX4 have been used to illustrate the *ePERF* analysis tool.

A comparative study and sensitivity study for the various aircraft configuration were conducted. In the comparative study, the results for the rotary wing modeling for vertical flight shows that the tiltrotor configuration with a very light disk loading as used in *eVTOL (B)* has a better hover performance compared the other configurations. While in the result for the drag modeling for cruise flight shows that the *eVTOL (A)* has the lowest drag due to its high aspect ratio wing, hence having the excellent L/D while *eVTOL (B)* has lowest power consumption in cruise at its respective best range velocity due to it has the lightest MTGW. In the mission-based modeling results, it shows that the *eVTOL (B)* has the lowest energy requirements as compared to the other configurations due to it has the lowest cruise power requirement.

As for the sensitivity study, several specific studies for the maximum takeoff gross weight, cruise velocity and defined ranges as well as defined battery capacities were conducted. These studies focus on the individual aspects and considerations for the eVTOL design and configurations. In the study of the variation of MTGW, result shows *eVTOL (B)* with 3175 kg, has the worst performance due its smaller wing and rotor area are optimized for lighter weight and one can not just arbitrarily increase the MTGW from 2177 to 3175 kg without re-size the aircraft geometry. The original *eVTOL (B)* with a MTGW of 2177 kg and its tiltrotor configuration show the best performance. In the study of the variation of cruise velocity, the results showed that the *eVTOL (A)* is able to achieve the greatest range while having the lowest cruising velocity.

On the other hand, the variation of both the *eVTOL (B)* and *eVTOL (B-3175)* are observed to have the highest cruising velocity due to its highly loaded wing. In the study of the variation of range, a similar result of *eVTOL (B)* is observed to have the lowest energy consumption to complete the various flight segments. In the final study of the variation of battery capacity, *eVTOL (B)* shows good range due to low cruise power required, but due to its lighter MTGW, *eVTOL (B)* will be unable to carry as much battery mass as compared to both *eVTOL (A)* or *(C).*

In summary, this study introduces the ePERF tool for various analysis for the eVTOL performance in the conceptual and preliminary design phase. The authors hope that the insights and findings presented here will be useful to aircraft designers and researchers in the design of the next generation of eVTOL aircrafts.

## Acknowledgements

The authors would like to thank Nanyang Technology University, Singapore for the financial support through grant 04INS000453C160. The first author acknowledges the support from Nanyang Technological University, Singapore for providing the Nanyang Presidential Graduate Scholarship.

## References

[1] S. A. C. S. Jayasooriya and Y. M. M. S. Bandara, “Measuring the Economic costs of traffic congestion,” *3rd Int. Moratuwa Eng. Res. Conf. MERCon 2017*, pp. 141–146, Jul. 2017, doi: 10.1109/MERCON.2017.7980471.

[2] C. Al Haddad, E. Chaniotakis, A. Straubinger, K. Plötner, and C. Antoniou, “Factors affecting the adoption and use of urban air mobility,” *Transp. Res. Part A Policy Pract.*, vol. 132, pp. 696–712, Feb. 2020, doi: 10.1016/J.TRA.2019.12.020.

[3] A. P. Cohen, S. A. Shaheen, and E. M. Farrar, “Urban Air Mobility: History, Ecosystem, Market Potential, and Challenges,” *IEEE Trans. Intell. Transp. Syst.*, vol. 22, no. 9, pp. 6074–6087, Sep. 2021, doi: 10.1109/TITS.2021.3082767.

[4] A. Straubinger, R. Rothfeld, M. Shamiyeh, K. D. Büchter, J. Kaiser, and K. O. Plötner, “An overview of current research and developments in urban air mobility – Setting the scene for UAM introduction,” *J. Air Transp. Manag.*, vol. 87, p. 101852, Aug. 2020, doi: 10.1016/J.JAIRTRAMAN.2020.101852.

[5] K. Khavarian and K. M. Kockelman, “Life-cycle Analysis of Electric Vertical Take-Off and Landing Vehicles.”

[6] S. P. Melo, F. Cerdas, A. Barke, C. Thies, T. S. Spengler, and C. Herrmann, “Life Cycle Engineering of future aircraft systems: the case of eVTOL vehicles,” *Procedia CIRP*, vol. 90, pp. 297–302, Jan. 2020, doi: 10.1016/J.PROCIR.2020.01.060.

[7] A. M. Stoll, J. Ben Bevirt, P. P. Pei, and E. V. Stilson, “Conceptual design of the joby S2 electric VTOL PAV,” *AIAA Aviat. 2014 -14th AIAA Aviat. Technol. Integr. Oper. Conf.*, pp. 16–20, 2014, doi: 10.2514/6.2014-2407.

[8] G. Droandi, M. Syal, and G. Bower, *Tiltwing Multi-Rotor Aerodynamic Modeling in Hover, Transition and Cruise Flight Conditions*. 2018.

[9] G. Wilke, “Aerodynamic Performance of Two eVTOL Concepts,” *Notes Numer. Fluid Mech. Multidiscip. Des.*, vol. 142, pp. 392–402, 2020, doi: 10.1007/978-3-030-25253-3_38/TABLES/10.

[10] J. M. Bustamante, C. A. Herrera, E. S. Espinoza, C. A. Escalante, S. Salazar, and R. Lozano, “Design and construction of a UAV VTOL in ducted-fan and tilt-rotor configuration,” *2019 16th Int. Conf. Electr. Eng. Comput. Sci. Autom. Control. CCE 2019*, Sep. 2019, doi: 10.1109/ICEEE.2019.8884533.

[11] A. Dikshit, T. Stokkermans, S. K. Y. Lim, and J. Wang, “Effect of Lifting Surface and Tail Configuration on the Aerodynamics and Flight Mechanics of VTOL Aircraft.” 2022.

[12] A. Bacchini and E. Cestino, “Electric VTOL Configurations Comparison,” *Aerosp. 2019, Vol. 6, Page 26*, vol. 6, no. 3, p. 26, Feb. 2019, doi: 10.3390/AEROSPACE6030026.

[13] C. Silva, W. Johnson, K. R. Antcliff, and M. D. Patterson, “VTOL Urban Air Mobility Concept Vehicles for Technology Development.”

[14] W. Johnson, C. Silva, and E. Solis, “Concept Vehicles for VTOL Air Taxi Operations.”

[15] A. Brown and W. L. Harris, “A vehicle design and optimization model for on-demand aviation,” *AIAA/ASCE/AHS/ASC Struct. Struct. Dyn. Mater. Conf. 2018*, no. 210049, 2018, doi: 10.2514/6.2018-0105.

[16] Electric VTOL News (2022). Beta Technologies ALIA. *evtol.news.* [Photo]. https://evtol.news/beta-technologies-alia/

[17] Electric VTOL News (2022). Joby S4. *evtol.news.* [Photo]. https://evtol.news/joby-s4

[18] Electric VTOL News (2022). Vertical Aerospace VX4 (production model). *evtol.news.* [Photo]. https://evtol.news/vertical-aerospace-VA-1X

[19] Uber, J. Holden, and N. Goel, “Fast-Forwarding to a Future of On-Demand Urban Air Transportation,” pp. 1–98, 2016, [Online]. Available: https://www.uber.com/elevate.pdf.

[20] Rotaru, C. & Todorov, M. (2017). Helicopter Flight Physics. In (Ed.), Flight Physics - Models, Techniques and Technologies. *IntechOpen*. https://doi.org/10.5772/intechopen.71516

[21] D. Raymer, “Aircraft Design: A Conceptual Approach, Sixth Edition,” *Aircr. Des. A Concept. Approach, Sixth Ed.*, Sep. 2018, doi: 10.2514/4.104909.